

---

EFDA–JET–CP(04)07-13

N.N. Gorelenkov, C.Z. Cheng, V.G. Kiptily, M.J. Mantsinen, S.E. Sharapov  
and JET-EFDA contributors

# Fast Ion Effects on Fishbones and $n = 1$ Kinks in JET Simulated by a Non-Perturbative NOVA-KN Code



# Fast Ion Effects on Fishbones and $n = 1$ Kinks in JET Simulated by a Non-Perturbative NOVA-KN Code

N.N. Gorelenkov<sup>1</sup>, C.Z. Cheng<sup>1</sup>, V.G. Kiptily<sup>2</sup>, M.J. Mantsinen<sup>3</sup>,  
S.E. Sharapov<sup>2</sup> and JET EFDA Contributors\*

<sup>1</sup>*Princeton Plasma Physics Laboratory, Princeton University, Princeton, NJ, 08543, USA*

<sup>2</sup>*EURATOM/UKAEA Fusion Association, Culham Science Centre, Abingdon, OX14 3DB, UK*

<sup>3</sup>*Helsinki University of Technology, Association Euratom-Tekes, Finland*

\* *See annex of J. Pamela et al, "Overview of JET Results",  
(Proc.20<sup>th</sup> IAEA Fusion Energy Conference, Vilamoura, Portugal (2004)).*

Preprint of Paper to be submitted for publication in Proceedings of the  
20th IAEA Conference,  
(Vilamoura, Portugal 1-6 November 2004)

“This document is intended for publication in the open literature. It is made available on the understanding that it may not be further circulated and extracts or references may not be published prior to publication of the original when applicable, or without the consent of the Publications Officer, EFDA, Culham Science Centre, Abingdon, Oxon, OX14 3DB, UK.”

“Enquiries about Copyright and reproduction should be addressed to the Publications Officer, EFDA, Culham Science Centre, Abingdon, Oxon, OX14 3DB, UK.”

## ABSTRACT.

A new global nonperturbative hybrid code, NOVA-KN, and its application to simulate resonant type modes in JET plasmas driven by energetic H-minority ions are presented. The NOVA-KN code employs the ideal MHD description for the background plasma and treats non-perturbatively the fast particle kinetic response, which includes the fast ion Finite Orbit Width (FOW) effect. In particular, the  $n = 1$  fishbone mode, which is in precession drift resonance with fast ions, is studied. The NOVA-KN code is applied to model the  $n = 1$  ( $f = 50 - 80\text{kHz}$ ) MHD activity observed recently in JET low density plasma discharges with high fast ion (H-minority) energy content generated during the ICRH. This  $n = 1$  MHD activity is interpreted as the instability of the  $n = 1$  precession drift frequency fishbone modes.

Low frequency  $n = 1$  MHD activity was observed in JET discharges with high fast-ion energy content comparable to or exceeding the energy content of the background plasma [1]. The frequency of such activity is between 50 and 80kHz. The period of sawteeth in those discharges was changed by a factor of five by controlling the plasma density. The energetic H-minority beta builds up strongly in low density plasmas, because the slowing down time of fast ions is inversely proportional to the electron density.

In this paper we report on the development and application of a new NOVA-KN (Kinetic Non-perturbative) hybrid code, which is an extension of the previously developed kinetic nonperturbative NOVA code in which fast ions were treated with Zero Orbit Width (ZOW) [2–4]. It uses the ideal MHD approximation for the background plasma and includes kinetic fast particle response non-perturbatively. The new version of NOVA-KN employs realistic approximation for fast ions including the Finite (arbitrary) Orbit Width (FOW) of fast ions. In its current version NOVA-KN includes only trapped hot ions. In general the mode frequencies of the resonant branche correspond to the combinations of characteristic trapped fast ion toroidal precession drift frequency,  $\omega d$ , and the bounce frequency  $\omega b$ . We apply NOVA-KN to study JET plasmas and show that the  $n = 1$  resonant and ideal branches can be unstable. Our results indicate that with the proper choices of hot ion population parameters the precession drift frequency resonant branch has frequency close to the one measured in experiments as was suggested in Ref.[5]. This requires the temperature of H-minority ions with Maxwellian distribution to be  $T_H \sim 1\text{MeV}$ . The mode structures and properties of such resonant branche are discussed.

## 1. EXPERIMENTAL OBSERVATIONS

For the analysis we choose one of JET discharges, #54305, which has a relatively low plasma density  $n_e \sim 2 \times 10^{13} \text{cm}^{-3}$ . Other plasma parameters in this shot are the equilibrium magnetic field at the geometrical center  $B_0 = 2.75\text{T}$ , the geometrical center at  $R_0 = 2:91\text{m}$ , and the plasma power is shown in Fig.1(a). This discharge reveals MHD activity in a new frequency range. Fig. 1 (b) clearly shows two types of plasma oscillations: 5080kHz and 1020kHz (around  $t \sim 12.5\text{sec}$ ) MHD activities, both with chirping frequencies on a millisecond time scale. Fast frequency chirping of

the former is different from the typical fishbone, whereas the latter has the downward chirping, more fishbone-like frequency evolution. Fourier analysis of these instabilities shows that the toroidal mode number is  $n = 1$ . For the interpretation of these observations it is critical to use realistic fast ion parameters such as the fast ion temperature measured by the diagnostic of the gamma ray emission due to fast proton interaction with different ion species [6]. In Fig.2(a) the measured gamma ray spectrum shows an emission peak at 4.4MeV, which is generated by minority ions at energies above 5MeV, whereas the time evolution of this peak amplitude is plotted in Fig.2(b). It reflects the correlation of the high energetic particle component density with the soft X-ray signal and is proportional to the density of high energy tail  $E_H > 5\text{MeV}$  ions. Detailed numerical analysis of this spectrum gives the effective temperature for the H-minority to be  $T_H \simeq 1(\pm 0.2)\text{MeV}$ .

## 2. NUMERICAL PROCEDURE

The detailed description of the numerical procedure will be published elsewhere while the basic set of equations is derived in Ref. [3]. The effect of fast ions is included through the perturbed pressure components perpendicular and parallel to the magnetic field, and the non-adiabatic parts of which are  $\delta p_{\perp} = m_h \int d^3v \mu B \hat{g}$ ,  $\delta p_{\parallel} = m_h \int d^3v 2(E - \mu B) \hat{g}$ , where  $\mu$  is the adiabatic invariant,  $B$  is the equilibrium magnetic field,  $E = v^2/2$ ,  $v$  is the absolute value of the hot ion velocity,  $m_h$  is the hot ion (H-minority, proton) mass,  $g$  is the nonadiabatic part of the perturbed hot ion distribution function. In this paper we will include only the trapped particle part of the nonadiabatic distribution function. For the function  $g$  we make use of the general expression from Ref. [7]

$$g = \sum_{m,p} E \bullet \frac{(\omega - \omega_*) G_{m,p} \partial F_h}{\omega - \bar{\omega}_d - p\omega_b \partial E} e^{-it\omega + im\theta - in\phi}, \quad (1)$$

where  $\omega_*$  is the H-minority drift frequency,  $G_{m,p}$  is the matrix of wave-particle interaction (see Ref.[3]),  $F_h$  is the H-minority equilibrium distribution function,  $\bar{\omega}_d$  is the bounce averaged toroidal precession drift frequency,  $\omega_b$  is the bounce frequency of ion periodic motion. In our previous work [5] FOW effects were kept via the ion drift motion characteristic frequencies, whereas matrix  $G$  was calculated in the ZOW limit. In addition the distribution function,  $F_h$ , was assumed isotropic. In this paper we compute the wave-particle interaction matrix  $G$  with FOW effects and with the following distribution function,

$$F_h = C e^{-E/T_H} e^{-(\lambda - \lambda_0)^2 / \Delta\lambda^2} (1 - \psi^2)^{2.2}, \quad (2)$$

where  $C$  is the normalization constant,  $T_H$  is the H-minority temperature, the Gaussian pitch angle distribution is centered at the magnetic axis, i.e. at  $\lambda = \lambda_0 = 1$ ,  $\lambda = \mu B_{ax}/E$ ,  $B_{ax}$  is the magnetic field at the magnetic axis,  $\psi$  is the poloidal magnetic flux within a given surface, normalized to its edge value. The pitch angle width is taken as  $\Delta\lambda = 0.05$ .

### 3. SIMULATIONS

To understand properties of resonant modes it is useful to show the spectrum of the Alfvén continuum as given in Fig.3(a) for the JET Pulse No: 54305 at  $t = 11$ sec in which the total beta was  $\beta_{\text{tot}} = 3.6\%$ . The  $q = 1$  surface is approximately at  $r/a \equiv \sqrt{\psi} = 0.6$ . Note, that the minor radius of the  $q = 1$  surface calculated with the respect to the normalized toroidal magnetic flux,  $\phi$ , is  $\sqrt{\phi} \sim 0.5$ . With the precession drift resonance, NOVA-KN finds two solutions. The first mode is the continuation of the ideal  $m = 1/n = 1$  mode (we call it I-mode), which has zero real frequency without hot ions and is located within the  $q = 1$  surface. The second solution is the resonant branch (called here R-mode) and has non-zero real frequency. The R-mode interacts with the continuum and typically experiences damping on it. Provided that the drive is strong enough such mode can be driven unstable by energetic ions due to the universal pressure gradient drive.

As expected the ideal kink mode is found unstable with NOVA-KN in the absence of hot ions, but is stabilized by the H-minority ions provided their temperature is high enough. At low temperature there is only one solution, I-mode. It stays unstable as the fast ion pressure is increased as shown in Fig.3(b), where the ratio of the H-minority temperature to the plasma ion plus electron temperature  $T_H = (T_i + T_e) = 6$ . All the frequencies here are normalized  $\Omega \equiv \omega q_a R_0 / v_{A0}$ , where  $q_a$  is the edge safety factor,  $v_{A0}$  is the central Alfvén velocity. The I-mode real frequency increases with the fast ion beta. At  $\beta_{H0} = \beta_{\text{tot}0} > 0.05$  this solution shows the same properties as the fishbone branch (R-mode): its frequency is close to the averaged precession drift frequency.

At higher temperature these two branches appear as separate solutions as shown in Fig.4(a) for  $T_H / (T_i + T_e) = 32$ . The R-mode frequency is an increasing function of H-minority temperature as shown in Fig. 4(b), and is almost proportional to the precession drift frequency of the H-minority population. It follows from Fig.4(a) that the I-mode is unstable at  $\beta_{H0} = \beta_{\text{tot}0} < 0.1$ . It is plausible that the ideal branch is responsible for the low end of the spectrum oscillations shown in Fig.1(b) at  $f = 10 - 20$ kHz. The frequency obtained from the NOVA-KN code is normalized to the Alfvén frequency, which for the considered plasma is about  $f_A = 130$ kHz, so that the I-mode solution should have mode frequency  $f_{\text{ideal}} \sim 1$ kHz according to Fig.4(a). Note that the plasma rotation frequency is about  $f_{\text{rot}} = 10$ kHz. Also we do not include the thermal ion diamagnetic frequency, which should increase the real frequency of the I-mode [8, 11]. If these effects are included, the I-mode frequency should account for the observed frequency of 10 – 20kHz.

The real part of the resonant branch frequency is determined by the characteristic particle frequencies. We plot the characteristic trapped hot particle drift motion frequencies corresponding to ions with the bounce point at the plasma vertical axis,  $\theta = \pi/2$ , and  $r = a/3$ , versus velocity normalized to the particle velocity at  $E_H = 0.54$ MeV ( $T_H / (T_i + T_e) = 32$ ) in Fig.5. In the same figure we show the velocity weighting function in the integrand of the perturbed pressure, which gives the maximum contribution from particles with velocities  $v/v_{H0} \sim 1.7$ . Such velocity corresponds to ions at the tail of the Maxwellian energy distribution, which have energy  $E_H = 1.56$ MeV. Thus, those energetic tail ions determine the frequency of the R-mode. One can see that for trapped ions

with bounce tip at  $0 = \pi/2$  the toroidal precession drift frequency is  $\Omega_d = 0.25$ . This value is close to the resonant mode frequency computed by the code,  $\Omega_{rR} = 0.21$  (see Fig.4(a)). One can see also from Fig.5 that the FOW effects do not change the toroidal precession significantly. On the other hand if the bounce resonance is included in the denominator of the perturbed pressure, the frequency of such resonant mode should have been  $W \sim 1.1$ , which is in the TAE frequency range and is much larger than the observed frequency.

The calculated real part of the R-mode frequency is  $\Omega_{rR} = 0.21$  (see Fig.4(a)) at  $T_H / (T_i + T_e) = 32$ , which corresponds to the measured value in the laboratory frame  $f = 20\text{kHz} + f_{\text{rot}} = 27\text{kHz}$  and  $T_H \sim 0.54\text{MeV}$ , which is the achieved computational limit for the FOW calculations. Fig.4(a) shows, as expected, that the R-mode frequencies in ZOW are very similar to the FOW results. This is due to, first, the toroidal precession drift frequencies are about the same, and, second, the minor radius of  $q = 1$  surface is large in the case we analyzed, so that the majority of fast ions are localized inside  $q = 1$  surface where FOW effects are not important. Thus if  $q = 1$  surface is near the magnetic axis we would expect the FOW effects to be significant as only part of particle orbit will be interacting with the mode.

In the case of ZOW we obtained  $\Omega_{rR} = 0.3$  for  $T_H / (T_i + T_e) = 60$  (or  $f \simeq 40\text{kHz} + f_{\text{rot}} = 50\text{kHz}$ ), which is consistent with observations and with the temperature of the H-minority at  $T_H = 1\text{MeV}$ .

One notes that the R-mode is stabilized at high particle energy  $T_H / (T_i + T_e) > 60$ . This is due to the mode frequency increase, which results in stronger continuum damping. Indeed the results of NOVA-KN can be used to find the continuum damping of the R-mode (see Fig.4(a)) by assuming that at each value of  $\beta_h = \beta_{\text{tot}}$  the imaginary part is given by  $\Omega_{iR} = \Omega_{i\text{cont}} + \Omega_{iH}$ , where  $\Omega_{iH} \sim \beta_h$  is the H-minority driving contribution to the growth rate of the R-mode. With this we find that  $\Omega_{i\text{cont}} = 0.043$  at  $\beta_h/\beta_{\text{tot}} = 0.2$  and is about 40% of the mode real frequency (for that one needs to extrapolate  $\Omega_{iR}(\beta_h/\beta_{\text{tot}})$  curve on figure 4(a) from  $\beta_h/\beta_{\text{tot}} > 0.24$  to  $\beta_h/\beta_{\text{tot}} = 0.2$  as the numerical solution at  $\beta_h/\beta_{\text{tot}} < 0.24$  should be discarded). It is also seen from Fig.4(a) that the critical pressure of H-minority to excite the R-mode is  $\beta_{\text{hcrit}}/\beta_{\text{tot}} = 0.2$ . The theory prediction for the precession drift frequency fishbone instability [2, 3, 9–11] is  $\beta_{\text{hcrit}} = \Omega_d/\pi q_a \simeq 0.68\%$  for  $\Omega_d$  taken at  $E_H = T_H = 0.54\text{MeV}$ . This is close to our result that  $\beta_h = 0.2\beta_{\text{tot}} = 0.72\%$  obtained for the same H-minority temperature. The theory also predicts that the continuum damping is proportional to the mode real frequency  $\Omega_{i\text{cont}} \simeq -\Omega_{rR}/q_a = 0.05$  (to be compared with the computed value of  $\Omega_{i\text{cont}} = 0.043$ ).

The observation that the continuum damping is proportional to the mode frequency is important and agrees with both numerical and experimental results. In Fig.1(b) at  $t \simeq 12.3\text{sec}$  the observed MHD activity frequency rises from 50kHz to 80kHz and results in the R-mode stabilization. The gamma ray spectrum peak signal increases at about that time (see Fig.2(b)), which may indicate the increase of the H-minority ion temperature.

Note that the increase in the mode frequency can be explained within the framework of the theory of the sawtooth effects on fast ions [12–14]. In that theory only low energy fraction among the trapped fast ions is redistributed within the  $q = 1$  surface. The threshold ion energy is determined



by the energy of fast ions, whose precession drift frequency equal to the inversed sawtooth crash time and typically reaches several hundreds keV in JET. It seems plausible that after the sawtooth crash the low energy part of the fast ion distribution function is depleted so that the average temperature is higher and the velocity space average of Eq.(1) results in higher mode frequency.

It is also important to note that the fast ion distribution function plays a major role in the R-mode frequency, which is supported by the numerical analysis. A broader pitch angle distribution and/or a higher value of  $\lambda_0$  (this is equivalent to changing the cyclotron resonance layer since  $\lambda_0 \sim R_{\text{res}}$ ) increases the frequency by up to 50%.

Radial mode structures we analyzed are shown in Fig. 6. The I-mode has a step like eigenmode structure at  $q = 1$  surface. On the other hand the R-mode has double step structure around  $q = 1$  surface with the width of the non-ideal layer proportional to the frequency of the mode. It is also seen that the mode structure changes significantly as the fast ion parameters evolve.

## SUMMARY

A new non-perturbative kinetic-MHD code NOVA-KN has been developed and is applied to study low frequency MHD activity observed in JET. The NOVA-KN code identifies the observed activity as the resonant fishbone mode which has the characteristic toroidal precession drift frequency of H-minority ions, and the result is in agreement with our initial studies [5]. Numerical simulations are able to find the continuum damping of the R-mode and the critical pressure sufficient to excite these modes. The R-mode continuum damping has been confirmed to be proportional to the mode frequency and explains the observed stabilization of such instability as its frequency increases.

## REFERENCES

- [1]. Mantsinen, M.J., Sharapov, S.E., Alper, B., Gondhalekar, A., McDonald, D.C., Plasma Phys. Control. Fusion, **42** (2000) 1291.
- [2]. Cheng, C.Z., Phys. Fluids **B 2** (1990) 1427.
- [3]. Cheng, C. Z., Phys. Reports, **211** (1992) 1.
- [4]. Cheng, C. Z., Fusion Technology **18** (1990) 443.
- [5]. Gorelenkov, N.N., Mantsinen, M.J., Sharapov, S.E., *et.al.* "Modeling of ICRH Hminority driven  $n = 1$  resonant modes in JET", 30th EPS Conference on Contr. Fusion and Plasma Phys., St. Petersburg, 7-11 July 2003 ECA Vol. 27A, P-2.100.
- [6]. Kiptily, V.G., Cecil, F.E., Jarvis, O.N., *et. al.*, "Nucl. Fusion, **42** (2002) 999.
- [7]. Gorelenkov, N.N., *et.al.*, Phys.Plasmas, **6** (1999) 2802.
- [8]. Coppi, B., Porcelli, F., Phys. Rev. Lett, **57** (1986) 2272.
- [9]. Chen, L., White, R.B., Rosenbluth, M.N., Phys. Rev. Lett., **52** (1984) 1122.
- [10]. White, R. B., Chen, L., Romanelli, F., Hay, R., Phys. Fluids, **28** (1985) 278.
- [11]. Wu, Yanlin, Cheng, C.Z., White, R.B., Phys. Plasmas **1** (1994) 3369.
- [12]. Kolesnichenko, Ya.I., Yakovenko, Yu.V., Nucl. Fusion **36** (1996) 159.

- [13]. Gorelenkov, N.N., Budny, R.V., Duong, H.H., Fisher, R.K., Medley, S.S., Petrov, M.P., Redi, M.H., Nuclear Fusion **37** (1997) 1053.
- [14]. Kolesnichenko, Ya.I., LUTSENKO, V.V., Yakovenko, Yu.V., Kamelander, G., Physics of Plasmas **4** (1997) 2544.

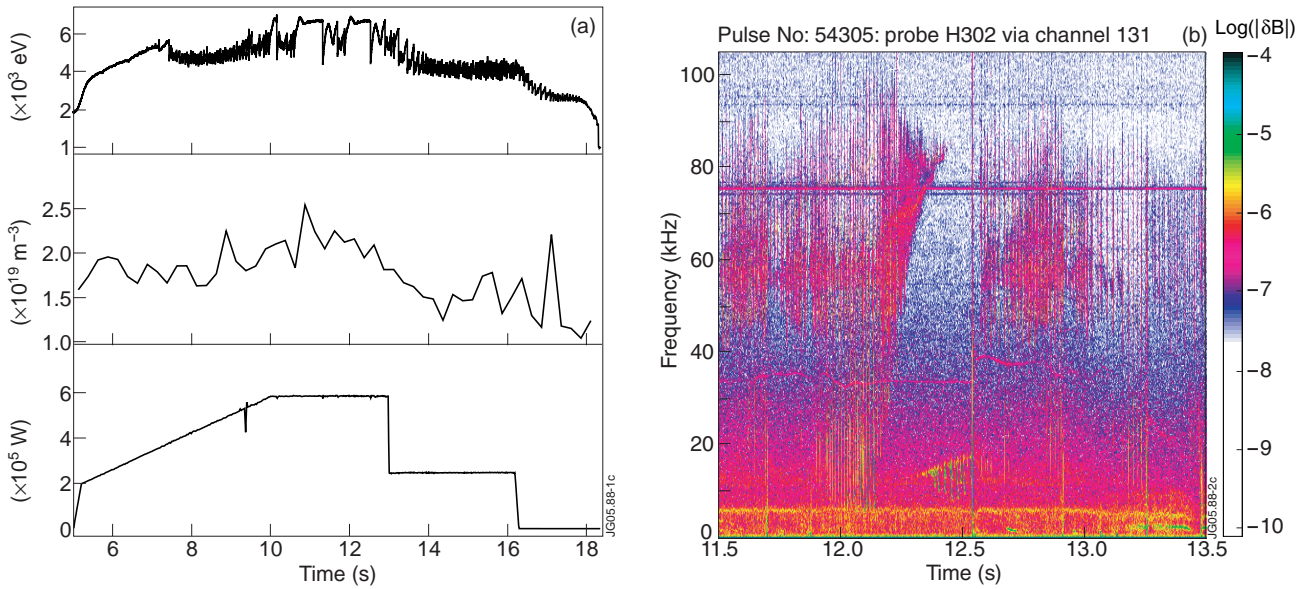


Figure 1: Plasma electron temperature, density and ICRH power in JET Pulse No: 54305 discharge are shown in figure (a). In figure (b), the evolution of the spectrum of the Mornov coil signal is presented for the frequency range  $f = 0 - 100\text{kHz}$ .

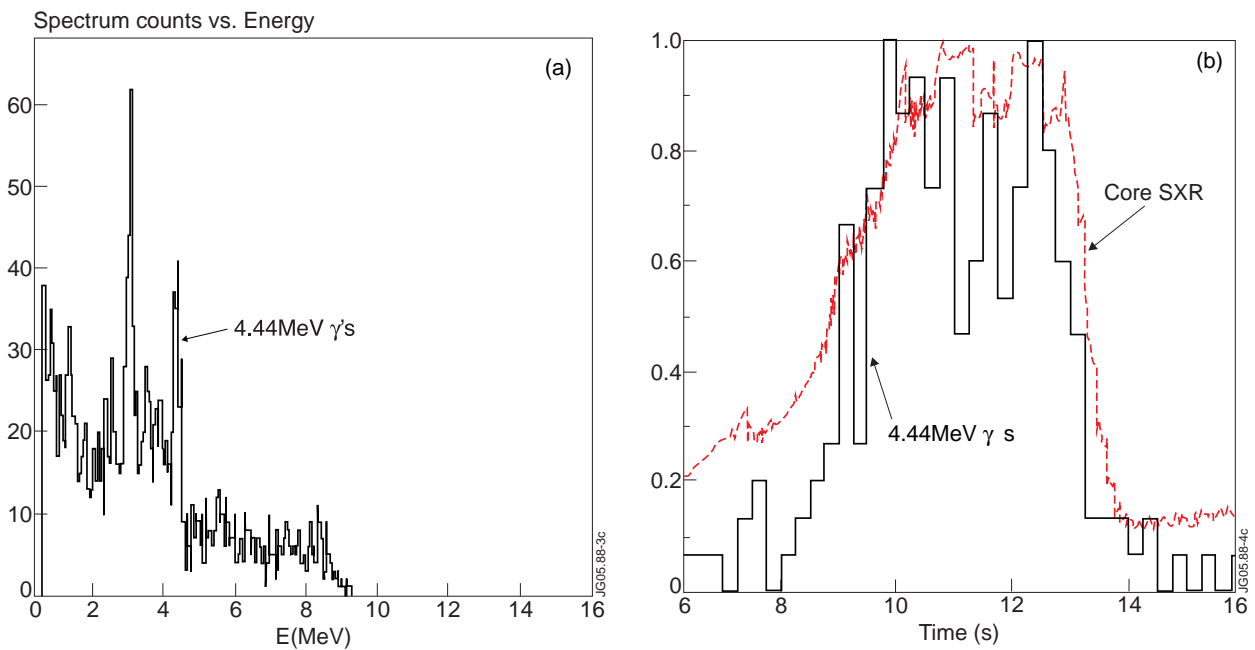


Figure. 2: Gamma ray spectrum for the JET Pulse No: 54305 (figure (a)) and the time evolution of its 4.4 MeV peak amplitude (figure (b)). Also shown in figure (b) is the evolution of the soft x-ray signal.

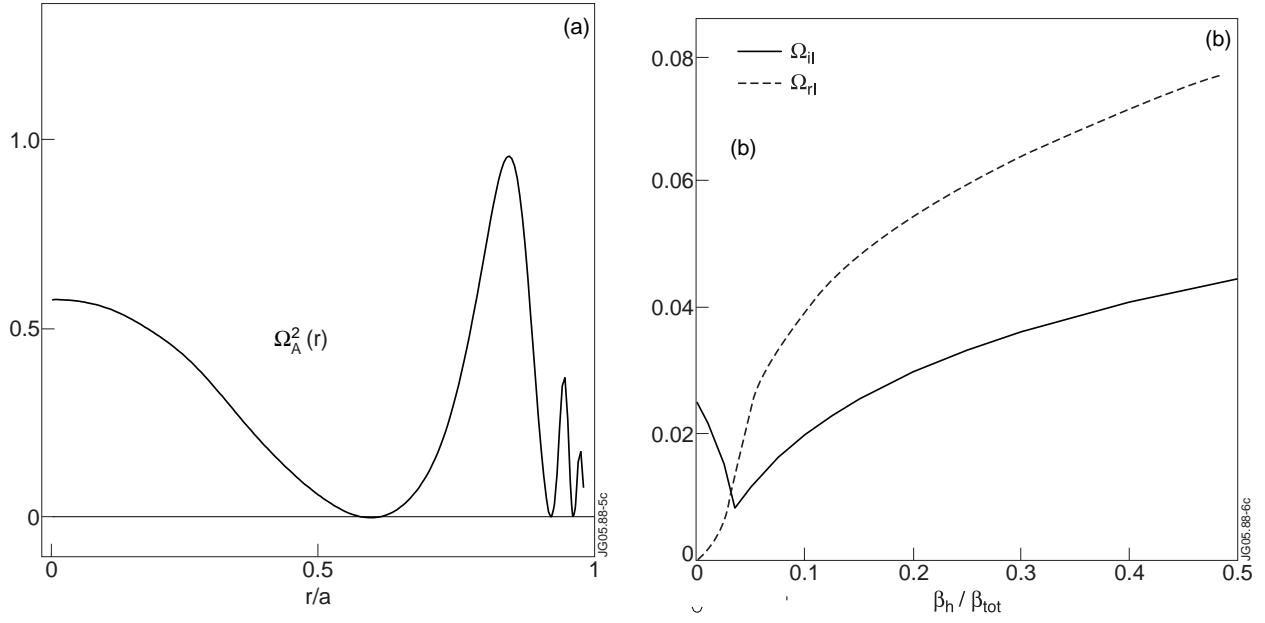


Figure 3: Alfvén continuum for  $n = 1$  (figure (a)) and ideal mode (I-mode) frequency (imaginary and real parts, subscripts  $i$  and  $r$ ) for the H-minority temperature  $T_H=(T_i+T_e) = 6$  (figure (b)). All the frequencies are normalized to the Alfvén frequency  $\Omega \equiv \omega q_a R_0 = v_{A0}$ .

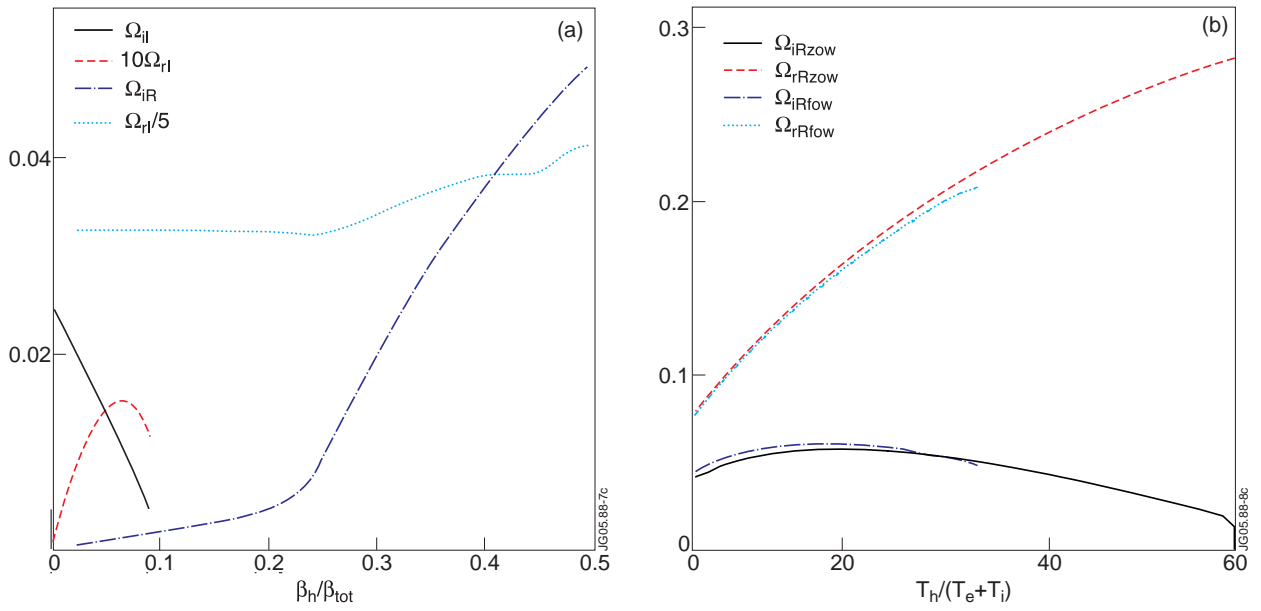


Figure 4: The ideal and fishbone (I- and R-) mode frequencies (subscripts  $I$  and  $R$ ) at  $T_H=(T_i+T_e) = 32$  (figure (a)). The real and imaginary parts of the R- mode frequency are shown as functions of H-minority temperature (figure (b)).

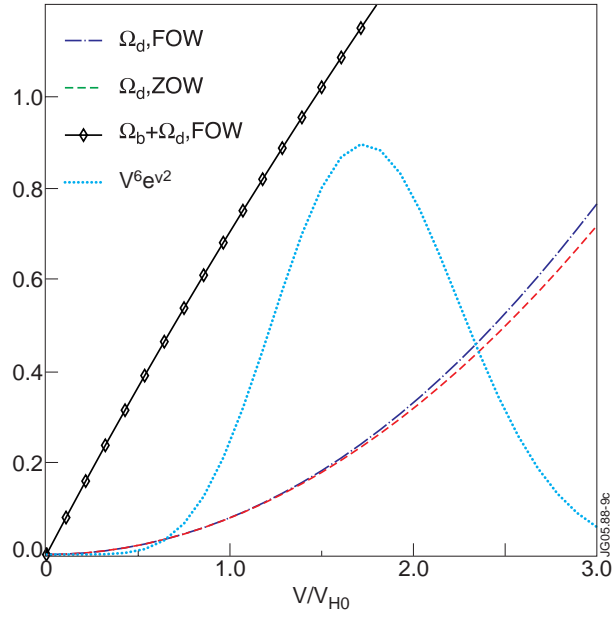


Figure 5: The H-minority ion characteristic frequencies as they appear in the denominator of Eq.(1) and the weighting factor, which is the integrand in the expression for the perturbed pressure. Velocity is normalized to the velocity of  $E_H \approx 0.54\text{MeV}$  H-minority ions.

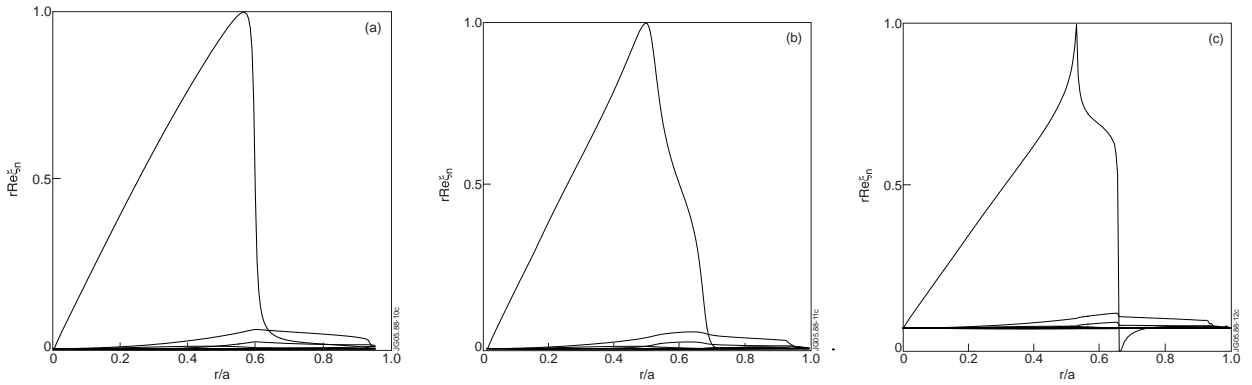


Figure 6: Radial structures of the resonant mode poloidal harmonics (the dominant harmonic has  $m = 1$  for all modes). In figure (a) the I-mode structure is given for  $\beta_h = \beta_{tot} = 0:002$  and  $T_H/(T_i + T_e) = 6$ . Figures (b) and (c) correspond to  $\beta_h = \beta_{tot} = 0:5$  and  $\beta_h = \beta_{tot} = 0:075$ , respectively for  $T_H/(T_i + T_e) = 32$ .